Published OnlineFirst March 10, 2009; DOI: 10.1158/0008-5472.CAN-08-1443

Research Article

Strong Smooth Muscle Differentiation Is Dependent on Myocardin Gene Amplification in Most Human Retroperitoneal Leiomyosarcomas

Gaëlle Pérot,[1,2] Josette Derré,[1,2] Jean-Michel Coindre,[3] Franck Tirode,[1,2] Carlo Lucchesi,[1,2] Odette Mariani,[1,2] Laure Gibault,[1,2] Louis Guillou,[4] Philippe Terrier,[5] and Alain Aurias[1,2]

[1]Genetics and Biology of Cancers, Institut Curie; [2]Institut National de la Santé et de la Recherche Médicale U830, Paris, France; [3]Department of Pathology, Institut Bergonié, Bordeaux, France; [4]Institut Universitaire de Pathologie, Centre Hospitalier Universitaire Vaudois, Lausanne, Switzerland; and [5]Department of Pathology, Institut Gustave Roussy, Villejuif, France

Abstract

Myocardin (MYOCD), a serum response factor (SRF) transcriptional cofactor, is essential for cardiac and smooth muscle development and differentiation. We show here by array-based comparative genomic hybridization, fluorescence *in situ* hybridization, and expression analysis approaches that *MYOCD* gene is highly amplified and overexpressed in human retroperitoneal leiomyosarcomas (LMS), a very aggressive well-differentiated tumor. *MYOCD* inactivation by shRNA in a human LMS cell line with *MYOCD* locus amplification leads to a dramatic decrease of smooth muscle differentiation and strongly reduces cell migration. Moreover, forced *MYOCD* expression in three undifferentiated sarcoma cell lines and in one liposarcoma cell line confers a strong smooth muscle differentiation phenotype and increased migration abilities. Collectively, these results show that human retroperitoneal LMS differentiation is dependent on MYOCD amplification/overexpression, suggesting that in these well-differentiated LMS, differentiation could be a consequence of an acquired genomic alteration. In this hypothesis, these tumors would not necessarily derive from cells initially committed to smooth muscle differentiation. These data also provide new insights on the cellular origin of these sarcomas and on the complex connections between oncogenesis and differentiation in mesenchymal tumors. [Cancer Res 2009;69(6):2269–78]

Introduction

Malignant soft-tissue sarcomas are a heterogeneous group of mesenchymal cancers accounting for ~1% of all malignant tumors in adult. These tumors are classified by pathologists according to their eventual line of differentiation. Among the well-differentiated sarcomas, tumors exhibiting a smooth muscle differentiation are classified as leiomyosarcomas (LMS) and correspond to 10% to 15% of soft-tissue sarcomas. They are generally localized to the retroperitoneum and less frequently to the limbs (1). These tumors have a poor prognosis and present very rearranged karyotypes, close to that observed in most undifferentiated pleomorphic sarcomas (2). These last undifferentiated sarcomas, which account for 5% of soft-tissue sarcomas (3), are preponderantly observed in limbs and are associated with a slightly better prognosis (1). Genetic similarities and a tendency to display an overlapping immunohistochemical phenotype suggest that both groups of tumors share common oncogenic pathways. Some genomic alterations are frequently observed in both groups, like deletion of chromosome 13, targeting the *RB1* gene (4), and deletion of 10q (5, 6), whereas 17p amplification is more specific of LMS. Here, we show that a target of this amplification likely corresponds to the gene encoding MYOCD, a transcriptional cofactor of serum response factor (SRF) regulating smooth muscle development and differentiation (7–9). Moreover, we show that MYOCD expression in sarcoma cell lines not only induces smooth muscle differentiation but also promotes cell migration, a feature that could be mediated by LPP induction. These results suggest that in these well-differentiated LMS, differentiation could be a consequence of an acquired genomic alteration, and that these tumors are not necessarily derived from cells initially committed to smooth muscle differentiation.

Materials and Methods

Tumor samples. Frozen samples and four fresh tumors were obtained from different pathology laboratories. All histologic slides were reexamined by the French Sarcoma Group: 19 tumors were classified as well-differentiated LMS and 17 tumors were classified as pleomorphic undifferentiated sarcomas. According to French law at the time of the study, the tumor samples were collected in agreement with the ANAES (Agence Nationale d'Accréditation et d'Evaluation en Santé) recommendations. Experiments were done in agreement with the Bioethics Law no. 2004-800 and the Ethics Charter from the National Institute of Cancer (INCa).

Cell line establishment and culture conditions. Sterile fragments from resected tumors LMS148, S100, S108, and S137 were minced in culture medium and then disaggregated by overnight incubation in collagenase (100 units/mL) at 37°C. Long-term culture (more than 70 passages were done) and standard harvesting procedures were used.

Sarcoma cell line culture was done in RPMI 1640 + GlutaMAX I (Life Technologies, Inc.) supplemented with 10% FCS (Abcys) and 1% penicillin-streptomycin (Life Technologies). HEK-293T cell line was cultured in DMEM + GlutaMAX I (Life Technologies) supplemented with 10% FCS (Abcys) and 1% penicillin-streptomycin (Life Technologies).

For the shRNA cell line culture, 0.4 μg/mL puromycin was added to this medium. For the pCDH1 infected cell line culture, 1 μg/mL (S100L, S108L, and S137L) or 2 μg/mL (LPS449) of puromycin were added to this medium.

For platelet-derived growth factor (PDGF)-BB experiments, LMS148L cells were seeded at a density of 1.5. 10^5 per well onto six-well plates and were cultured for 48 h in medium without FCS. Then cells were treated with human recombinant PDGF-BB (R&D) for 24 h at a concentration of

Note: Supplementary data for this article are available at Cancer Research Online (http://cancerres.aacrjournals.org/).

Accession number: The Affymetrix data observed on the 32 human tumors and on the LMS148L cell line have been deposited in the EMBL-EBI database (http://www.ebi.ac.uk/) and are accessible through accession no. E-MEXP-1922.

Requests for reprints: Alain Aurias, Institut Curie, 26 rue d'Ulm, Paris 75005, France. Phone: 33-1-42-34-66-79; Fax: 33-1-42-34-66-30; E-mail: alain.aurias@curie.fr.

doi:10.1158/0008-5472.CAN-08-1443

Published OnlineFirst March 10, 2009; DOI: 10.1158/0008-5472.CAN-08-1443

100 ng/mL. LMS148L cells cultured in the absence of PDGF-BB were used as control. Smooth muscle–related gene expression was then assessed by real-time PCR from three independent experiments.

Immunohistochemistry. Immunohistochemistry was done on paraffin blocks according to the method described previously (2). For cell lines, cells were seeded at a density of 10^5 per well onto two-well Lab-Tek slides (Nunc). Twenty-four hours later, cells were fixed with cold acetone solution for 10 min. After blocking with 20% FCS (Abcys), 2% bovine serum albumin (Sigma) in Tris buffer solution for 30 min, cells were incubated with the primary antibody and then treated in the same manner as the paraffin sections. Experiments were realized with the same antibodies used for Western blot except for α-smooth muscle actin (SMA; M0851, DAKO). Anti-calponin and anti-transgelin antibodies were used at a dilution of 1:1,000; anti-SMA antibody and anti-caldesmon antibodies were used at a dilution of 1:50.

Human array-based comparative genomic hybridization and image analysis. Genomic DNA was isolated using a standard phenol-chloroform extraction protocol. Array-based comparative genomic hybridization (array-CGH) experiments were done with a DNA microarray developed in our laboratory. Three thousand eight hundred seventy-four BAC/PAC DNAs (BACPAC Resources Center, Children's Hospital Oakland Research Institute) were spotted in triplicate on Ultragaps slides (Corning). These clones cover up the whole genome with a resolution of 1 Mb. The probes were prepared and hybridized as previously described (10). The data were analyzed by a software developed at Institut Curie.[6] Cyanine-5/cyanine-3 ratios >2 were considered as amplifications, and ratios >1.2 and <0.8 were considered as gains and losses, respectively.

Fluorescence *in situ* hybridization. Metaphase spreads were obtained by standard procedures. For frozen tissues, 5-μm-thick tumor sections were used. Probes used correspond to BAC RP11-746E8, which overlaps the *MYOCD* genomic sequence (located in band 17p12), and BAC RP11-388C12, located in band 17q25.3, as a control probe. Fluorescence *in situ* hybridization (FISH) was done as previously described (10). Photographs were obtained using a Zeiss Axioplan 2 microscope, a Photometrics Quantix CCD camera, and the SmartCapture v2 Digital Scientific software.

Transcriptome analysis. Total RNA was extracted from frozen tumor samples or from cell line with TRIzol reagent (Life Technologies). RNA was then purified using the RNeasy Min Elute Cleanup Kit (Qiagen) according to the manufacturer's procedures. RNA quality was checked on an Agilent 2100 bioanalyzer (Agilent Technologies). Samples were then analyzed on Human Genome U133 Plus 2.0 array (Affymetrix) according to the manufacturer's procedures. All microarray data were simultaneously normalized using the GCRMA algorithm (11). Hierarchical clusterings were done using the dChip software (average linkage method, rank correlation distance metric). For Welch test, a significant variation corresponds to fold changes >1.5 or ≤1.5, with $P < 0.05$ (Benjamini-Hochberg P-value correction).

Real-time quantitative reverse transcription-PCR. Reverse transcription and real-time PCR were done as previously described (12). We used the TaqMan Gene Expression assays provided by Applied Biosystems. The assay IDs were as follows: Hs00538076_m1 for *MYOCD*, Hs00182371_m1 for *SRF*, Hs00189021_m1 for *CALD*, Hs00154543_m1 for *CNN1*, Hs00162558_m1 for *TAGLN*, Hs00426835_g1 for *ACTA2* (SMA), Hs00252979_m1 for *MRTF-A*, Hs00539161_s1 for *MRTF-B*, Hs00944352_m1 for *LPP*, and Hs99999902_m1 for *RPLP0*. To normalize the results, we used the *RPLP0* gene as a reference gene. Human tumor data were normalized against a reference tumor for which *MYOCD* expression is intermediate (LMS77). The results were calculated as described by De Preter and colleagues (13).

Western blot. Total proteins of tumors were extracted by crushing frozen tumor samples in 8 mol/L urea (Interchim Uptima). Radioimmunoprecipitation assay buffer is used for cell line total proteins extraction. The primary antibodies and dilutions used in this study are as follows: antibodies to MYOCD (1:200; A-13, Santa Cruz Biotechnology), CNN1 (1:10,000; C2687, Sigma-Aldrich), SM22α (TAGLN; 1:10,000; ab14106, Abcam), hCALD (1:1,000; M3557, DAKO), α-SMA (1:400; A2547, Sigma-Aldrich), GKLF (KLF4; 1:500; H-180, Santa Cruz Biotechnology), PDGF (1:100; Ab-1, 101-116, Calbiochem), LPP (1:500; Ab63621, Abcam), hemagglutinin (HA; 1:10,000; 12CA5, Roche), or β-actin (1:10,000; Sigma-Aldrich). Secondary antibodies were horseradish peroxidase conjugated: antirabbit IgG (1:3,000; NA934, Amersham), antimouse IgG (1:3,000; NA931V, Amersham), or antigoat IgG (1:10,000; sc-2020, Santa Cruz Biotechnology). Western blot images were acquired with a Fujifilm luminescent image LAS-1000plus analyzer. They were analyzed with Image Gauge V4.0 software, which allowed us to normalize protein of interest expression data to β-actin expression values.

siRNA. SiGENOME SMARTpool siRNA (Dharmacon) directed against myocardin (MYOCD) and siCONTROL Non-Targeting siRNA pool (Dharmacon) were used to perform *MYOCD* expression knockdown experiments in LMS148L. Negative Control siRNA Alexa Fluor 488 (Qiagen) and siControl Human Cyclophilin B siRNA (Dharmacon) were used as transfection controls. LMS148L cells were seeded at a density of 1.2×10^5 per well onto six-well plates 24 h before transfection. The cells were washed with Opti-MEM (Life Technologies) and then incubated for 5 h at 37°C in 60 μL of Opti-MEM and 15 μL of Oligofectamine reagent (Invitrogen) containing 100 pmol of the siRNA of interest. The same steps were reproduced for the second transfection at 3 d. Each transfection was done twice for all siRNAs. For real-time PCR experiments, gene expressions in cell lines transfected with *MYOCD* specific siRNA were compared with those in cell lines transfected with the nontargeting siRNA control. A mean of inhibition percentages was then calculated for each time point for each gene.

shRNA. RNA*intro* kit for pSM2 retroviral shRNAmir (RHS3601) with three shRNAmir directed against *MYOCD* (shRNA1.14: RHS1764-9697831; shRNA1.8: RHS1764-9403778 and shRNA1.3: RHS1764-9100135) and a nonsilencing shRNAmir control (RHS1703; Open Biosystems) were used to perform a stable inhibition of *MYOCD* expression. The vectors were prepared and transfected in the LMS148L cell line as recommended by the manufacturer. The selection of the stable transfected cells was done 48 h after transfection using 0.4 μg/mL puromycin. *MYOCD* expression inhibition was checked by real-time PCR and only the cells transfected with shRNA1.14 and shRNA1.8 presented a significative inhibition. Specific *MYOCD* shRNA 1.14 subclones were then established by limiting dilution (one cell every three wells, as a mean) onto four 96-well plates. Forty subclones were then tested by real-time PCR, and finally two subclones were selected according to their *MYOCD* expression inhibition (sh1.14C1 and sh1.14C2). For real-time PCR experiments, gene expressions in shRNA cell lines (sh1.8, sh1.14, sh1.14C1, and sh1.14C2) were examined thrice and compared with those in the cell line transfected with the nonsilencing shRNA control (NT), also examined thrice. A mean of inhibition percentages was then calculated for each shRNA for each gene.

Immunofluorescence. Cells were seeded in duplicate at a density of 10^4 per well onto eight-well Lab-Tek slides (Nunc). Twenty-four hours later, cells were fixed with a 3.7% paraformaldehyde solution for 20 min. They were then permeabilized with 0.01% SDS in PBS 1× for 10 min. After each treatment step, cells were washed with PBS 1×. After blocking with 10% FCS in PBS 1× for 20 min, cells were incubated with anti-TAGLN or anti-CNN1 antibodies at a dilution of 1:500 and 1:1,000, respectively, in PBS 1× with 10% FCS for 1 h at room temperature. Then, cells were incubated with rabbit immunoglobulins/TRITC or mouse immunoglobulins/FITC (DAKO) at a dilution of 1:50 and 1:400, respectively, in PBS 1× with 10% FCS for 1 h at room temperature. Immunofluorescence experiments were done with the same antibodies used for Western blot, and photographs obtained as described above in FISH section.

Migration assays. The cell migration activity was assayed in Boyden chambers with polycarbonate membrane of 8.0-μm pore size (Corning). Cells were suspended to a final concentration of 5×10^4/mL in medium with 0.5% FCS and were added to the upper compartment. Medium, with 0.5% FCS or 10% FCS as a chemoattractant, was added to the plate well and cells were incubated for 24 h at 37°C. The cells on the upper surface of the filter were removed by wiping with cotton swabs, and the cells on the lower surface were stained with crystal violet. The cells that had invaded to the lower surface areas were photographed (Coolpix 8400, Nikon) under a microscope (Eclipse TS100, Nikon).

[6] http://bioinfo.curie.fr/HumanCGHarray/

Published OnlineFirst March 10, 2009; DOI: 10.1158/0008-5472.CAN-08-1443

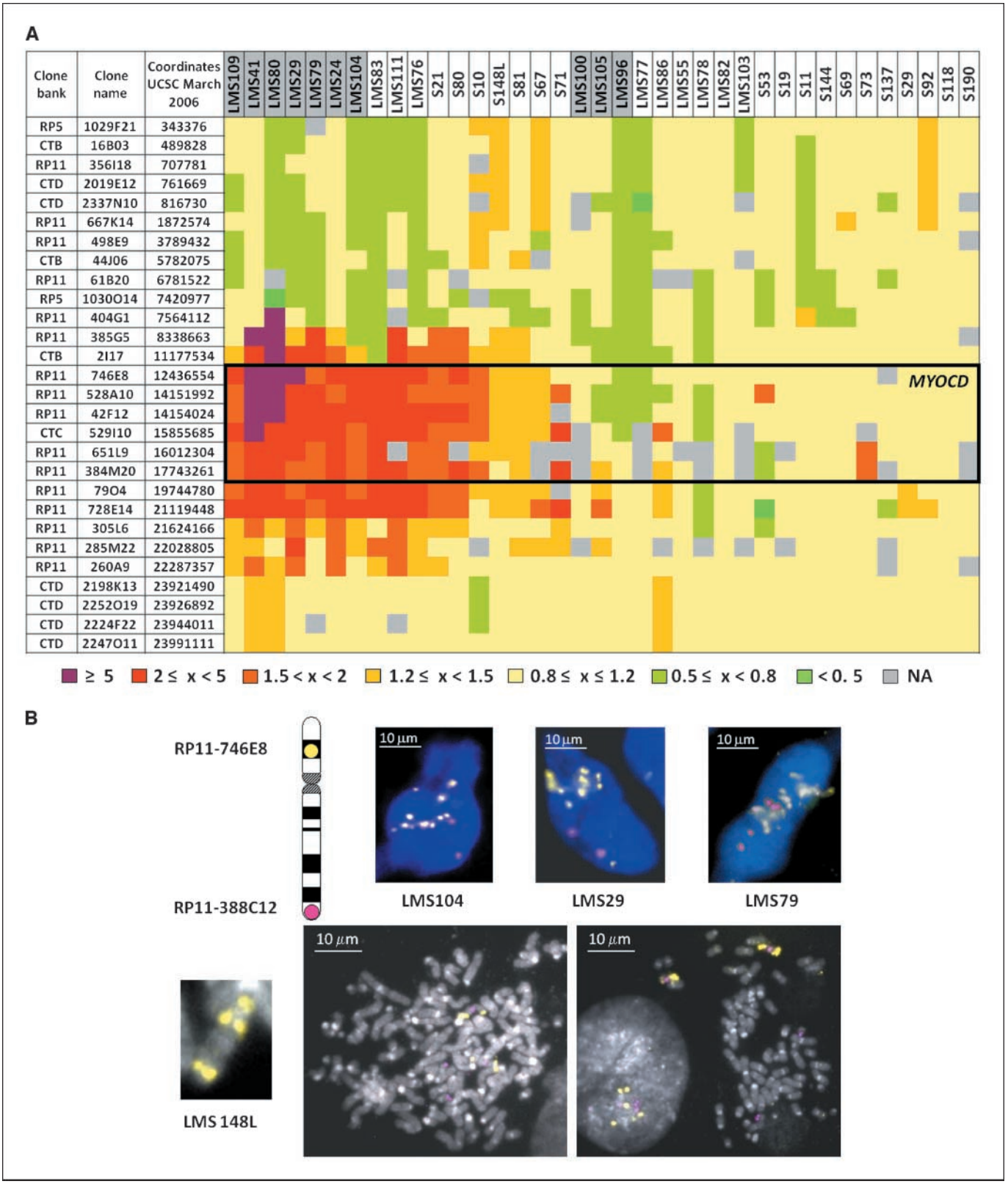

Figure 1. Genomic amplification of the 17p11.2-17p12 region. *A,* CGH results on 28 BAC-PAC clones covering the major part of 17p chromosome. The names of these clones and their genomic locations are indicated on the left. The names of studied tumors are indicated at the top, and retroperitoneal tumors are shaded in gray. The genomic status (tumor DNA/normal DNA ratio) of each tumor for each locus is indicated by a color code in filled squares, as defined at the bottom. Position of *MYOCD* gene is indicated as well as the minimal common region of amplification (*open black box*). *B,* FISH on frozen sections of tumors LMS104, LMS29, and LMS79 and on metaphase spreads from the LMS148L cell line. The *MYOCD* probe corresponds to BAC RP11-746E8 and is labeled with Cy3-dUTP (*yellow*). The control locus, corresponding to the telomeric clone RP11-388C12 on the long arm of chromosome 17, is labeled with Cy5-dUTP (*pink*). Genomic amplification of this locus is observed in all samples. *Inset,* the *MYOCD* gain in the LMS148L cell line is enlarged. *Bar,* 10 μm.

Published OnlineFirst March 10, 2009; DOI: 10.1158/0008-5472.CAN-08-1443

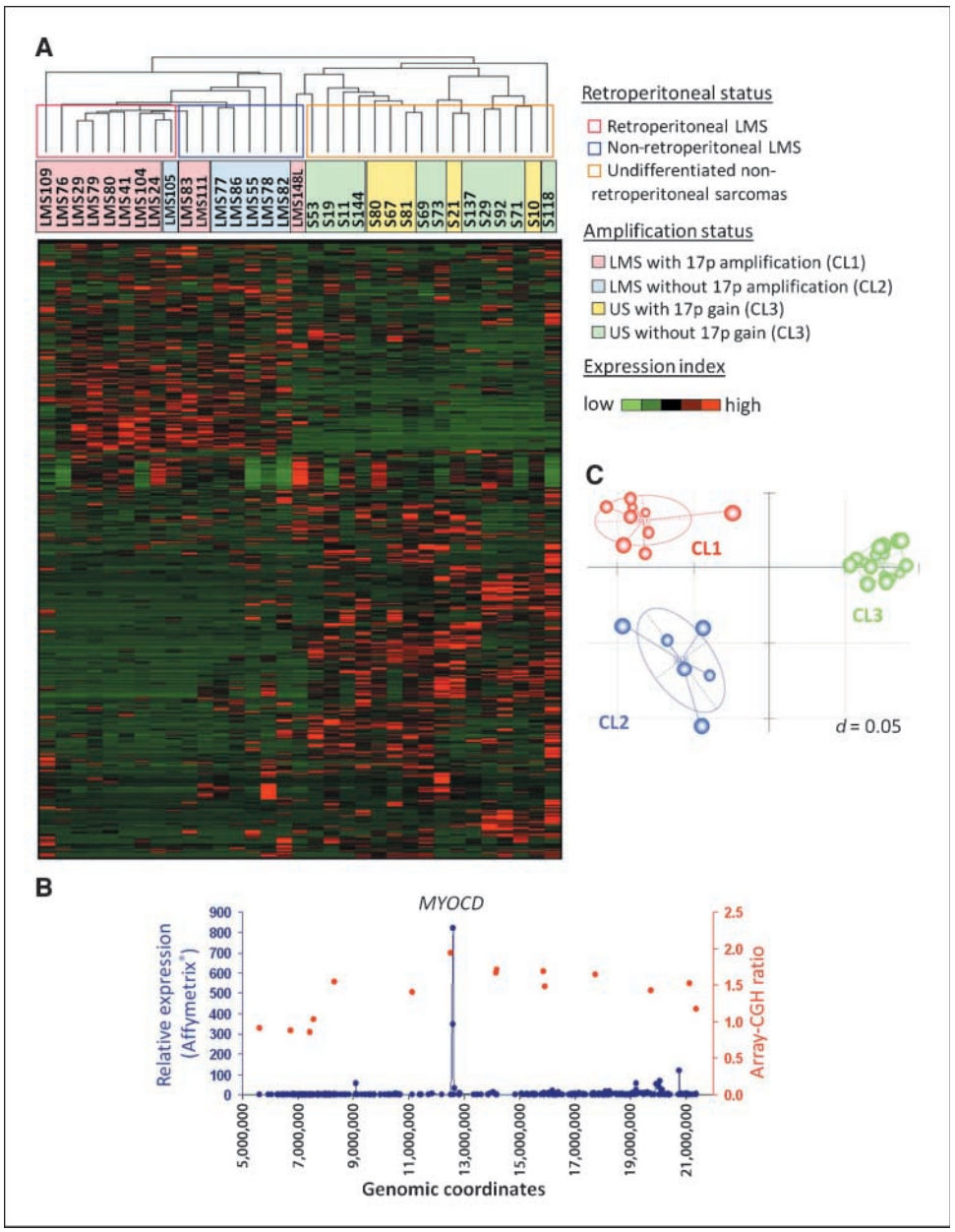

Figure 2. Gene expression profile of LMS and undifferentiated sarcomas. *A,* unsupervised hierarchical clustering was done by dChip software using Affymetrix data obtained for the most variant genes (interquartile range >2). The retroperitoneal status of the tumors is indicated by open colored boxes on the cluster tree. The 17p amplification status of the tumors is represented on the tumor's name. *B,* the median ratio of expression for each probe set in the major part of the chromosome 17p, between LMS with 17p amplification and undifferentiated sarcomas, is represented by the blue curve. In the same manner, array-CGH mean ratio for each BAC locus, between the two groups of tumors, was calculated and is represented by the red curve. Genomic position of the probe sets is presented on the abscissa. *C,* between-group analysis of LMS with 17p amplification (CL1), LMS without amplification (CL2), and undifferentiated sarcomas (CL3).

For measurement of cell migration by wound healing assay, confluent cells were wounded with a plastic micropipette tip having large orifice. The experiment was done twice in duplicate for each cell lines. Photographs of three randomly selected points along each wounded area were taken just after wounding and after 24, 32, and 48 h (Coolpix 8400, Eclipse TS100, Nikon).

Lentiviral constructs and infections. For lentiviral expression, HA-tagged MYOCD-encoding sequence obtained from GeneCopoeia (EX-E0450-Lv06) was amplified by PCR with added 5′-end *Xba*1 and 3′-end *Swa*1 restriction enzyme sites and then was cloned between these restriction sites in the lentiviral pCDH1 vector (SBI). Viral particles were produced in HEK-293T cells transfected with appropriate packaging plasmids by the calcium phosphate method. Viral supernatants were supplemented with 8 μg/mL polybrene for infection and puromycin was added 24 h later.

Results

Tumor samples. A series of 37 samples were analyzed (36 frozen tumors and 1 cell line). Their main clinical and pathologic data are indicated in Supplementary Table S1. These tumors were extensively characterized by immunohistochemistry (Supplementary Fig. S1). Tumors were classified by pathologists of the French Sarcoma Group as well-differentiated LMS according to their morphologic features and when they exhibit a positive immunolabeling for all smooth muscle–related genes. As shown in Supplementary Table S1, our series of frozen tumors consists of 19 well-differentiated LMS and 17 pleomorphic undifferentiated or poorly differentiated sarcomas. All these tumors were analyzed by array-CGH and they all present complex rearranged karyotypes. Transcriptomes of 16 of 19 LMS and 16 of 17 undifferentiated sarcoma samples were analyzed using U133Plus 2.0 Affymetrix arrays. For this purpose, data were normalized using the GCRMA algorithm.

Most well-differentiated LMS present an amplification of the 17p11.2-p12 genomic region. In the present sarcoma series, increased copy number or amplification were recurrently observed

Published OnlineFirst March 10, 2009; DOI: 10.1158/0008-5472.CAN-08-1443

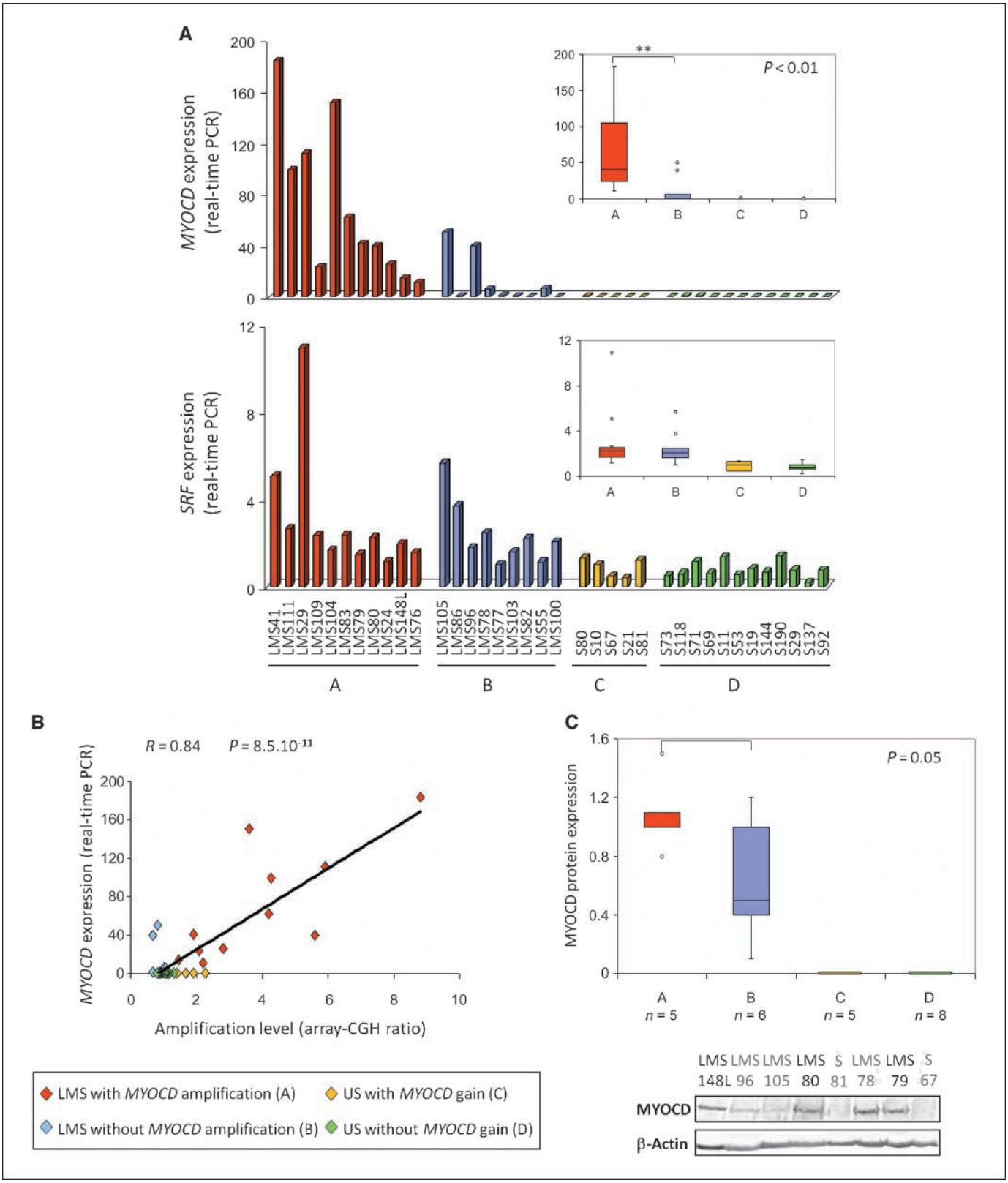

Figure 3. MYOCD overexpression in amplified LMS. *A, MYOCD* and *SRF* expression levels estimated by real-time PCR. The tumor groups are indicated: *group A,* LMS with 17p amplification; *group B,* LMS without 17p amplification; *group C,* undifferentiated sarcomas with 17p gain; *group D,* undifferentiated sarcomas without 17p gain. Boxplots corresponding to each bar chart are shown on the right. *B,* relative expression level of *MYOCD* estimated by real-time PCR correlates with the genomic amplification level obtained by array-CGH experiments (Pearson's correlation). *C,* boxplot analysis of MYOCD protein expression between the different tumor groups (*P* value using Student's *t* test). *Bottom right,* a representative Western blot with anti-MYOCD antibody.

Published OnlineFirst March 10, 2009; DOI: 10.1158/0008-5472.CAN-08-1443

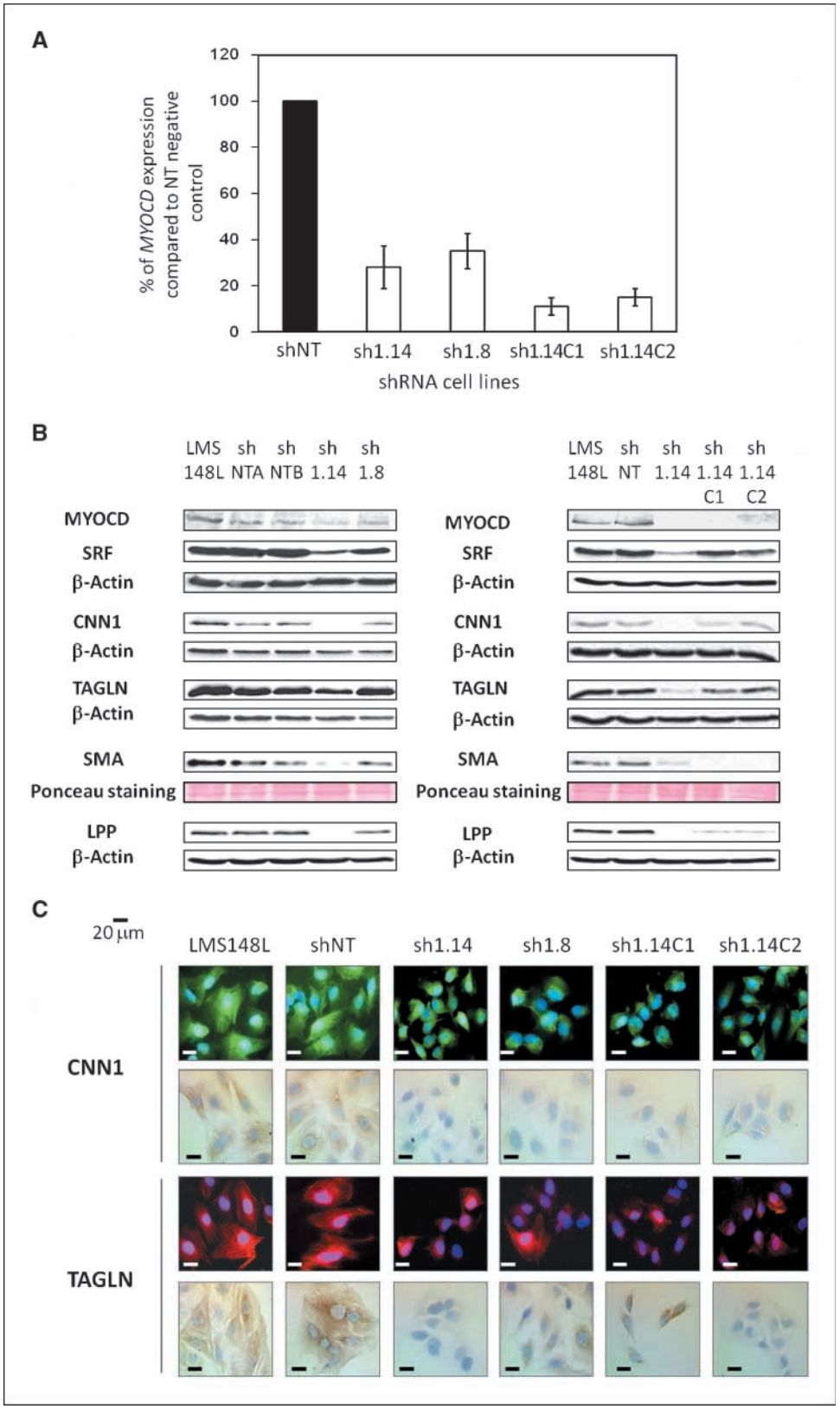

Figure 4. Inhibition of *MYOCD* expression by shRNA. *A,* the *MYOCD* expression level in cells transfected with two specific *MYOCD* shRNAs (sh1.14 and sh1.8) and in the two derived subclones (sh1.14C1 and sh1.14C2) is estimated by real-time PCR. These data were compared with those of cells transfected with a nonsilencing shRNAmir control (*shNT*). *Columns,* mean percentages obtained for triplicate experiments; *bars,* SD. *B,* immunoblotting of total protein extracts from LMS148L and shRNA-treated cells revealed by CNN1, TAGLN, SMA, and LPP antibodies and by an anti–β-actin antibody. For SMA Western blots, Ponceau staining is shown as a loading control. *C,* CNN1 and TAGLN immunofluorescence and immunocytochemistry experiments done on LMS148L and shRNA-treated cells. *Bar,* 20 μm.

by array-CGH for clones corresponding to 17p11.2-17p12 loci (Fig. 1*A*), with a minimal common region of gain at coordinates chr17:12,436,554–17,743,261 in the Human March 2006 Assembly at UCSC. This overrepresentation of 17p chromosome was essentially observed in LMS (10 LMS among 16 amplified tumors) and particularly in those with retroperitoneal occurrence: 8 of 11 retroperitoneal LMS do present this amplification, whereas only 2 of 8 non-retroperitoneal LMS have the 17p amplification. Moreover,

Published OnlineFirst March 10, 2009; DOI: 10.1158/0008-5472.CAN-08-1443

high-level amplification of 17p chromosome (array-CGH ratio > 2) was exclusively observed in LMS. Genomic amplification was confirmed by fluorescence *in situ* hybridization (FISH) on frozen tissue sections from 8 tumors and on metaphase spreads from the LMS148L cell line, with a probe corresponding to the most amplified locus (clone RP11-746E8). High copy number of this locus was confirmed in all tumors (Fig. 1*B*) when compared with a 17q control probe (RP11-388C12 BAC clone). In metaphase from LMS148L, a cell line established from a LMS, a complex rearrangement was observed on a derivative chromosome 17 with a gain of the RP11-746E8 locus (Fig. 1*B*).

***MYOCD* gene is the most overexpressed gene in the minimal amplified region.** An unsupervised hierarchical clustering was done with dChip software using normalized transcriptome data. As shown in Fig. 2*A*, two main tumor clusters corresponding to the well-differentiated LMS on one hand and to the undifferentiated sarcomas on the other hand were observed. Each of these two clusters is subdivided, and for example, in the LMS cluster, most of the amplified tumors are grouped together. In a first step, we analyzed the relative expression of genes from the major part of the 17p chromosome between LMS with amplification and undifferentiated sarcomas. As shown in Fig. 2*B*, two probe sets exhibit a dramatic increase in relative expression: Both correspond to a gene that encodes the MYOCD protein, a SRF transcription cofactor regulating smooth muscle differentiation (7–8, 14). Moreover, this gene is contained in clone RP11-746E8 and thus located in the region with higher amplification level. These results strongly suggest that this gene could be a major target of the amplicon. In a second step, we performed a Welch test to determine the genes that are differentially expressed between LMS and undifferentiated sarcomas. The *MYOCD* gene is detected among the top 100 genes and is the first from the amplified 17p region, a result which strengthens the previous hypothesis. When we compared by Welch test LMS with amplification and undifferentiated sarcomas, *MYOCD* gene is the third most significantly differentially expressed gene (and the first from the 17p amplicon). Finally, we performed a supervised analysis by between-group analysis (15) of LMS with 17p amplification (CL1), LMS without amplification (CL2), and undifferentiated sarcomas (CL3). The three clusters are well separated (Fig. 2*C*). *MYOCD* gene is the most specific gene of LMS with 17p amplification group (CL1), whereas this gene is not specific of LMS without 17p amplification group (CL2; data not shown). These analyses show that even if *MYOCD* is expressed in CL2, it is much more expressed in CL1 tumors with 17p amplification. All these data reinforce the hypothesis that the *MYOCD* gene is a major target of 17p amplification.

***MYOCD* overexpression is strongly correlated to its genomic amplification and to smooth muscle–related gene expression.** To confirm the consequences of its genomic amplification, we tested *MYOCD* expression by quantitative real-time PCR (Fig. 3*A*). The data are presented as relative expressions compared with a moderately differentiated LMS (LMS77, differentiation scoring of 6). In LMS with 17p amplification, *MYOCD* expression is higher than in other LMS ($n = 20$; $P < 0.01$, Student's t test), confirming the role of its amplification in its expression. Moreover, a strong Pearson's correlation between genomic amplification of *MYOCD* locus and its RNA expression ($n = 37$, $R = 0.84$, $P < 0.001$) is observed (Fig. 3*B*). Nevertheless, to precisely appreciate the contribution of the amplification to the *MYOCD* expression, the correlation coefficient has also been calculated after exclusion of nonamplified LMS. In this case, this correlation was stronger ($n = 28$, $R = 0.87$, $P < 0.001$; data not shown), suggesting again in the amplified LMS a major role for amplification of the *MYOCD* gene in its expression. We then performed a Western blot analysis on most samples (24 of 37 tumors). Results of MYOCD expression normalized by β-actin level between the different groups of tumors are indicated in Fig. 3*C*, which shows a significant higher MYOCD expression in LMS with 17p amplification, compared with other LMS ($P = 0.05$, Student's t test). As expected, smooth muscle–related genes (SMA, CNN1, TAGLN, and CALD) are expressed at high level only when MYOCD and SRF are expressed (Fig. 3*A*; Supplementary Fig. S2*A* and *B*).

Undifferentiated or poorly differentiated sarcomas do not express *MYOCD* (Fig. 3*A–C*; Supplementary Fig. S3*A*). Nevertheless, as shown in Supplementary Fig. S3*A*, five of them exhibit a moderate gain of the *MYOCD* locus (S10, S21, S67, S80, and S81), but express only, and at low level, one or two smooth muscle–related genes (Supplementary Table S1; Supplementary Fig. S2*A* and *B*). Few data on transcriptional regulation of *MYOCD* are available, but one explanation for the discrepancy between genomic gain of *MYOCD* and absence of clear smooth muscle differentiation could be related to expression of *MYOCD* inhibitors. For example, S10, S80, and S67 exhibit a high expression level of *KLF4* (Supplementary Fig. S3*B*), a gene recently described as a smooth muscle differentiation inhibitor (16), both by down-regulating *MYOCD* expression and by interfering with SRF/MYOCD complex to prevent its association with smooth muscle–related gene promoters. In the same manner, S81 and S80 express high level of *PDGFB* (Supplementary Fig. S3*B*), which is implicated in the same differentiation repressive pathway (16, 17). In accordance with this hypothesis, treatment of the LMS148L cell line with human recombinant PDGF-BB leads to a strong decrease of *MYOCD* gene expression and of the smooth muscle–related genes (Supplementary Fig. S3*C*).

***In vitro MYOCD* inactivation leads to a decrease of smooth muscle differentiation.** It has been well demonstrated that MYOCD forced expression in different cellular models induces smooth muscle–related gene expression (7, 8, 18–21). The strong correlation between *MYOCD* gene expression and its

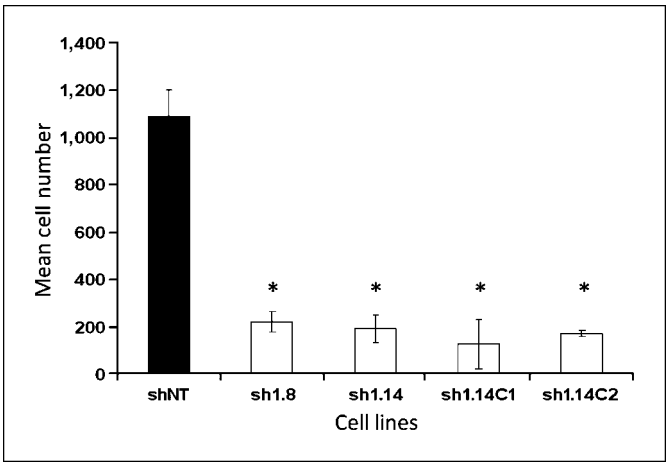

Figure 5. Effect of *MYOCD* expression inhibition by shRNA on cell migration. Mean number of cells that had invaded to the lower surface areas of Boyden chambers after 24 h of culture. *Columns,* mean for each cell line, established from experiments done in duplicate; *bars,* SD. *, $P < 0.05$ (Student's t test).

Published OnlineFirst March 10, 2009; DOI: 10.1158/0008-5472.CAN-08-1443

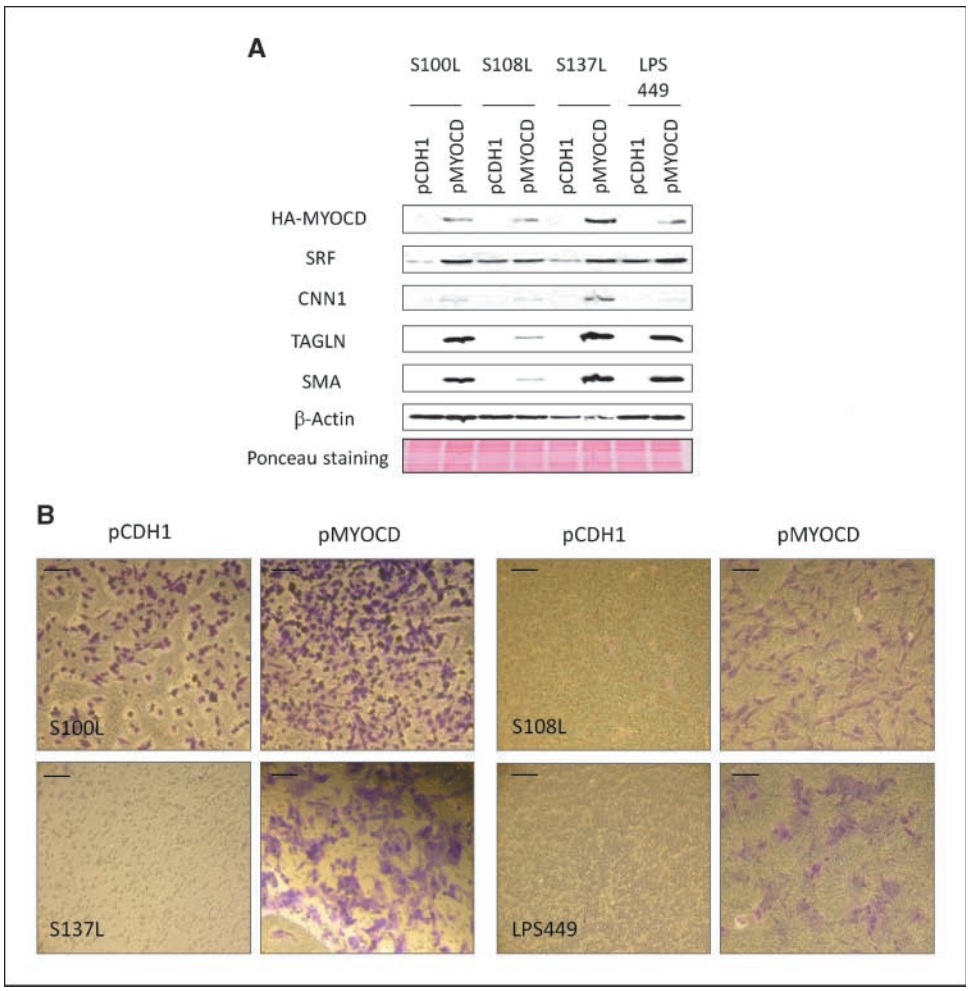

Figure 6. Forced MYOCD expression in different cell lines. *A,* HA-MYOCD, SRF, CNN1, TAGLN, SMA, and β-actin protein expression levels obtained by Western blot in cells infected with an empty pCDH1 vector or with a pCDH1 MYOCD expression vector (pMYOCD). Ponceau staining is shown as a loading control. *B,* effect of forced MYOCD expression on cell migration. Representative photographs of two independent experiments. Cells from each cell line were cultured on the permeable membrane (0.8-μm pores) of Boyden chambers in medium with 0.5% FCS. Medium with 10% FCS as a chemoattractant was added to the plate well. After 24 h, cells on the membrane of the lower chamber were stained with crystal violet and were photographed. *Bar,* 100 μm.

amplification, observed in most well-differentiated LMS, fits well with these data. To confirm the involvement of *MYOCD* amplification in LMS differentiation, we first transitorily inhibited *MYOCD* in LMS148L using specific SMARTpool siRNAs. As indicated above, this cell line presents a complex rearrangement of 17p11.2-p12 (Fig. 1*B*), associated with an overrepresentation of the *MYOCD* locus and with a strong expression of the *MYOCD* gene together with the other smooth muscle–related genes (Fig. 3; Supplementary Fig. S2*A* and *B*). In this siRNA experiment, a strong inhibition of *MYOCD* was obtained, associated with a parallel dramatic decrease of smooth muscle–related gene expression, particularly at day 4 when the inhibition of *MYOCD* is maximal (Supplementary Fig. S4). To more precisely document the link between MYOCD expression and smooth muscle differentiation, we established stable LMS148L cell lines transfected with *MYOCD* specific shRNAs (sh1.14 and sh1.8) and with a nontargeting shRNA (NT). We then isolated two different subclones from LMS148L transfected with shRNA1.14 (sh1.14C1 and sh1.14C2). As shown in Fig. 4*A* and *B*, an important inhibition of *MYOCD* gene and smooth muscle–related proteins was observed in the sh1.8 and sh1.14 cell lines and in the sh1.14C1 and sh1.14C2 subclones. These data were confirmed by immunocytochemistry (Fig. 4*C*): Indeed, in shRNA cell lines, a dramatic disorganization of the smooth muscular fibers is observed, with a perinuclear relocalization of the remaining TAGLN and CNN1 proteins. All these results strongly support the lead role of *MYOCD* gene amplification in producing the features of smooth muscle differentiation observed in LMS.

***MYOCD* inhibition leads to a decrease of cell migration.** MYOCD family members have been described as potential regulators of cell migration (9). To document if MYOCD expression could modulate migration in a LMS context, we performed a series of migration assays for 24 hours in Boyden chambers on shRNA-treated cell lines. As shown in Fig. 5 and Supplementary Fig. S5, shRNA control cells (shNT) were observed in the lower chamber. This migration was almost completely abolished in *MYOCD* shRNA cell lines (sh1.8, sh1.14, sh1.14C1, and sh1.14C2). We then performed a wound healing experiment on the same cell lines (Supplementary Fig. S6). In LMS148L and in control cells, the wound was healed at 24 h, and the cells were confluent at 32 hours. In contrast, the *MYOCD* shRNA cell lines did not show wound healing at 32 hours and were not completely confluent at 48 hours.

It has been recently shown that LPP promotes smooth muscle cell migration (22, 23) and that its expression is regulated by MYOCD (22, 24). Indeed in our series, *LPP* is overexpressed in LMS compared with undifferentiated sarcomas (Supplementary Fig. S7), and its expression is decreased when *MYOCD* expression is inhibited by shRNAs in LMS148L (Fig. 4*B*). These results suggest

that, in a LMS context, increased migration could be due to the up-regulation of *LPP* expression by *MYOCD* overexpression.

***MYOCD* forced expression in undifferentiated sarcoma cell lines leads to a robust smooth muscle differentiation and increases cell migration.** We then performed forced MYOCD expression experiments, using a lentiviral vector, in three undifferentiated sarcoma cell lines (S100L, S108L, and S137L) and in a liposarcoma cell line (LPS449). As shown in Fig. 6*A* and Supplementary Fig. S8, forced HA-tagged MYOCD expression was obtained, leading to a strong smooth muscle differentiation in all cell lines, as previously observed in different cellular models (7, 8, 18–21).

We also show that MYOCD up-regulation in sarcoma cell lines strongly promotes migration (Fig. 6*B*) and LPP expression (Supplementary Fig. S8). These results fit well with those described above after *MYOCD* inhibition by shRNAs.

Discussion

It is generally accepted that most oncogenic processes are associated with a progressive loss of the cell differentiation status, conferring a more proliferative and aggressive phenotype (25–31). Nevertheless, LMS have a very poor prognosis, in spite of a strong differentiation, suggesting that in this cellular context, differentiation and proliferation are not necessarily antinomic. This peculiar situation could be favored by the fact that smooth muscle cells do not reach a terminal differentiation but retain a remarkable plasticity, converting from a quiescent well-differentiated to a highly proliferative state. In some physiologic instances, smooth muscle cells may even grow in a maintained differentiated contractile phenotype (32–34).

Rearrangements of 17p chromosome region have been described in constitutionnal disorders (35, 36) or in malignancies (37–39), especially in LMS (2, 40). The present analysis not only confirms the occurrence of a highly recurrent 17p11.2-17p12 amplification in LMS but also shows that this amplification is predominantly observed in tumors located at the retroperitoneum. As previously proposed (41), these data suggest not only that this region contains key genes involved in LMS biology but also that the genetics of LMS could be linked to the localization of the tumor.

Our approach, combining array-CGH and transcriptome analysis, shows that the *MYOCD* gene is localized in the region with the highest amplification level, and that it is the most differentially expressed gene between LMS with the 17p amplification and undifferentiated sarcomas. Furthermore, its expression is hugely correlated with its level of genomic amplification. MYOCD protein, a SRF transcription cofactor, regulates smooth muscle differentiation (7, 8, 14). Its inactivation by siRNA and shRNAs in the LMS148L cell line leads to a dramatic decrease of smooth muscle–related genes. Its forced expression in different cellular models (7, 8, 18–21) and in four sarcoma cell lines (our results) induces smooth muscle–related gene expression. Collectively, these data strongly suggest that *MYOCD* is a major target of the amplification, and that smooth muscle differentiation in these LMS could be acquired as a consequence of a chromosomal rearrangement. Our results also suggest that these retroperitoneal tumors do not necessarily derive from cells initially committed to smooth muscle differentiation, but that they could stem from undifferentiated mesenchymal cells, compelled to this differentiation through *MYOCD* locus amplification.

LMS without 17p amplification, essentially occurring in limbs, express *MYOCD* and smooth muscle–related genes. It is noticeable that these LMS present also a higher expression level of *MRTF-A* and *MRTF-B* than LMS with *MYOCD* amplification (Supplementary Fig. S9). These genes encode MYOCD-related proteins, which, in association with SRF, could also induce smooth muscle differentiation (42–44) and could be implicated in the biology of these limb tumors. Thus, these limb LMS could derive from cells already committed to smooth muscle differentiation. As previously proposed (45), these tumors could be of vascular origin, with a constitutive expression of the *MYOCD* and *MRTF* genes, or from cells carrying a more subtle alteration leading to an indirect activation of these genes.

Finally, we show that *MYOCD* expression is strongly associated with the migration ability of the cells, whatever the cellular context. This feature could be due to the up-regulation of *LPP*, a MYOCD target involved in smooth muscle cell migration (22–24). *MYOCD* overexpression could thus be involved in the particularly high rate of metastases observed in LMS.

In conclusion, our data show that a chromosomal rearrangement, acquired during oncogenesis, could both compel tumor cells to reach a strong specific differentiation and participate in the metastasis process.

Disclosure of Potential Conflicts of Interest

No potential conflicts of interest were disclosed.

Acknowledgments

Received 4/17/2008; revised 12/17/2008; accepted 1/16/2009; published OnlineFirst 3/10/09.

Grant support: Institut National de la Santé et de la Recherche Médicale, Institut Curie, INCa (PL007), Conticanet network and Fondation de France. The construction of the human BAC-array was supported by grants from the Carte d'Identité des Tumeurs program of the Ligue Nationale Contre le Cancer. G. Pérot was supported by fellowships from the Ministère de l'Enseignement Supérieur et de la Recherche and from the Association pour la Recherche sur le Cancer, and L. Gibault by grants from Paris-Descartes University.

The costs of publication of this article were defrayed in part by the payment of page charges. This article must therefore be hereby marked *advertisement* in accordance with 18 U.S.C. Section 1734 solely to indicate this fact.

We thank X. Sastre-Garau (Department of Pathology, Institut Curie, Paris, France), D. Ranchère (Department of Pathology, Centre Léon Bérard, Lyon, France), and Y.M. Robin (Department of Pathology, Centre Oscar Lambret, Lille, France) for providing tumor samples; F. Larousserie for help with immunohistochemistry protocol; F. Pédeutour (Laboratory of Solid Tumor Genetics, University Hospital, Nice, France) for the generous gift of LPS449 cell line; and D. Williamson for critical reading of the manuscript.

References

1. Fletcher CDM, Unni KK, Mertens F, editors. World Health Organisation classification of tumours. Pathology and genetics of tumours of soft tissue and bone. Lyon: IARC Press; 2002.
2. Derré J, Lagacé R, Nicolas A, et al. Leiomyosarcomas and most malignant fibrous histiocytomas share very similar comparative genomic hybridization imbalances: an analysis of a series of 27 leiomyosarcomas. Lab Invest 2001;81:211–5.
3. Fletcher CD. The evolving classification of soft tissue tumours: an update based on the new WHO classification. Histopathology 2006;48:3–12.
4. Chibon F, Mairal A, Fréneaux P, et al. The RB1 gene is the target of chromosome 13 deletions in malignant fibrous histiocytoma. Cancer Res 2000;60:6339–45.
5. Otaño-Joos M, Mechtersheimer G, Ohl S, et al. Detection of chromosomal imbalances in leiomyosarcoma by comparative genomic hybridization and interphase cytogenetics. Cytogenet Cell Genet 2000;90:86–92.
6. Hu J, Rao UN, Jasani S, Khanna V, Yaw K, Surti U. Loss

Published OnlineFirst March 10, 2009; DOI: 10.1158/0008-5472.CAN-08-1443

of DNA copy number of 10q is associated with aggressive behavior of leiomyosarcomas: a comparative genomic hybridization study. Cancer Genet Cytogenet 2005;161:20–7.
7. Du KL, Ip HS, Li J, et al. Myocardin is a critical serum response factor cofactor in the transcriptional program regulating smooth muscle cell differentiation. Mol Cell Biol 2003;23:2425–37.
8. Wang Z, Wang DZ, Pipes GC, Olson EN. Myocardin is a master regulator of smooth muscle gene expression. Proc Natl Acad Sci U S A 2003;100:7129–34.
9. Pipes GC, Creemers EE, Olson EN. The myocardin family of transcriptional coactivators: versatile regulators of cell growth, migration, and myogenesis. Genes Dev 2006;20:1545–56.
10. Vincent-Salomon A, Gruel N, Lucchesi C, et al. Identification of typical medullary breast carcinoma as a genomic sub-group of basal-like carcinomas, a heterogeneous new molecular entity. Breast Cancer Res 2007;9:R24.
11. Wu Z, Irizarry RA, Gentleman R, Murillo FM, Spencer F. A model based background adjustment for oligonucleotide expression arrays. J Am Stat Assoc 2004;99:909–17.
12. Tirode F, Laud-Duval K, Prieur A, Delorme B, Charbord P, Delattre O. Mesenchymal stem cell features of Ewing tumors. Cancer Cell 2007;11:421–9.
13. De Preter K, Speleman F, Combaret V, et al. Quantification of MYCN, DDX1, and NAG gene copy number in neuroblastoma using a real-time quantitative PCR assay. Mod Pathol 2002;15:159–66.
14. Wang Z, Wang DZ, Hockemeyer D, McAnally J, Nordheim A, Olson EN. Myocardin and ternary complex factors compete for SRF to control smooth muscle gene expression. Nature 2004;428:185–9.
15. Culhane AC, Perrière G, Considine EC, Cotter TG, Higgins DG. Between-group analysis of microarray data. Bioinformatics 2002;18:1600–8.
16. Liu Y, Sinha S, McDonald OG, Shang Y, Hoofnagle MH, Owens GK. Kruppel-like factor 4 abrogates myocardin-induced activation of smooth muscle gene expression. J Biol Chem 2005;280:9719–27.
17. Holycross BJ, Blank RS, Thompson MM, Peach MJ, Owens GK. Platelet-derived growth factor-BB-induced suppression of smooth muscle cell differentiation. Circ Res 1992;71:1525–32.
18. Chen J, Kitchen CM, Streb JW, Miano JM. Myocardin: a component of a molecular switch for smooth muscle differentiation. J Mol Cell Cardiol 2002;34:1345–56.
19. Wang DZ, Olson EN. Control of smooth muscle development by the myocardin family of transcriptional coactivators. Curr Opin Genet Dev 2004;14:558–66.
20. Yoshida T, Sinha S, Dandré F, et al. Myocardin is a key regulator of CArG-dependent transcription of multiple smooth muscle marker genes. Circ Res 2003;92:856–64.
21. van Tuyn J, Knaän-Shanzer S, van de Watering MJ, et al. Activation of cardiac and smooth muscle-specific genes in primary human cells after forced expression of human myocardin. Cardiovasc Res 2005;67:245–55.
22. Gorenne I, Jin L, Yoshida T, et al. LPP expression during *in vitro* smooth muscle differentiation and stent-induced vascular injury. Circ Res 2006;98:378–85.
23. Majesky MW. Organizing motility: LIM domains, LPP, and smooth muscle migration. Circ Res 2006;98:306–8.
24. Petit MM, Lindskog H, Larsson E, et al. Smooth muscle expression of lipoma preferred partner is mediated by an alternative intronic promoter that is regulated by serum response factor/myocardin. Circ Res 2008;103:61–9.
25. Ghafar MA, Anastasiadis AG, Chen MW, et al. Acute hypoxia increases the aggressive characteristics and survival properties of prostate cancer cells. Prostate 2003;54:58–67.
26. Helczynska K, Kronblad A, Jögi A, et al. Hypoxia promotes a dedifferentiated phenotype in ductal breast carcinoma *in situ*. Cancer Res 2003;63:1441–4.
27. Abelev GI, Lazarevich NL. Control of differentiation in progression of epithelial tumors. Adv Cancer Res 2006;95:61–113.
28. Cheuk W, Chan JK. Advances in salivary gland pathology. Histopathology 2007;51:1–20.
29. van Staveren WC, Solís DW, Delys L, et al. Human thyroid tumor cell lines derived from different tumor types present a common dedifferentiated phenotype. Cancer Res 2007;67:8113–20.
30. Edsjö A, Holmquist L, Påhlman S. Neuroblastoma as an experimental model for neuronal differentiation and hypoxia-induced tumor cell dedifferentiation. Semin Cancer Biol 2007;17:248–56.
31. Mariani O, Brennetot C, Coindre JM, et al. JUN oncogene amplification and overexpression block adipocytic differentiation in highly aggressive sarcomas. Cancer Cell 2007;11:361–74.
32. Owens GK. Regulation of differentiation of vascular smooth muscle cells. Physiol Rev 1995;75:487–517.
33. Owens GK, Kumar MS, Wamhoff BR. Molecular regulation of vascular smooth muscle cell differentiation in development and disease. Physiol Rev 2004;84:767–801.
34. Hellstrand P, Albinsson S. Stretch-dependent growth and differentiation in vascular smooth muscle: role of the actin cytoskeleton. Can J Physiol Pharmacol 2005;83:869–75.
35. Inoue K, Dewar K, Katsanis N, et al. The 1.4-Mb CMT1A duplication/HNPP deletion genomic region reveals unique genome architectural features and provides insights into the recent evolution of new genes. Genome Res 2001;11:1018–33.
36. Park SS, Stankiewicz P, Bi W, et al. Structure and evolution of the Smith-Magenis syndrome repeat gene clusters, SMS-REPs. Genome Res 2002;12:729–38.
37. Forus A, Weghuis DO, Smeets D, Fodstad O, Myklebost O, Geurts van Kessel A. Comparative genomic hybridization analysis of human sarcomas. II. Identification of novel amplicons at 6p and 17p in osteosarcomas. Genes Chromosomes Cancer 1995;14:15–21.
38. Frühwald MC, O'Dorisio MS, Dai Z, et al. Aberrant hypermethylation of the major breakpoint cluster region in 17p11.2 in medulloblastomas but not supratentorial PNETs. Genes Chromosomes Cancer 2001;30:38–47.
39. van Dartel M, Cornelissen PW, Redeker S, et al. Amplification of 17p11.2 approximately p12, including PMP22, TOP3A, and MAPK7, in high-grade osteosarcoma. Cancer Genet Cytogenet 2002;139:91–6.
40. El-Rifai W, Sarlomo-Rikala M, Knuutila S, Miettinen M. DNA copy number changes in development and progression in leiomyosarcomas of soft tissues. Am J Pathol 1998;153:985–90.
41. Wolf M, Tarkkanen M, Hulsebos T, et al. Characterization of the 17p amplicon in human sarcomas: microsatellite marker analysis. Int J Cancer 1999;82:329–33.
42. Wang DZ, Li S, Hockemeyer D, et al. Potentiation of serum response factor activity by a family of myocardin-related transcription factors. Proc Natl Acad Sci U S A 2002;99:14855–60.
43. Du KL, Chen M, Li J, Lepore JJ, Mericko P, Parmacek MS. Megakaryoblastic leukemia factor-1 transduces cytoskeletal signals and induces smooth muscle cell differentiation from undifferentiated embryonic stem cells. J Biol Chem 2004;279:17578–86.
44. Selvaraj A, Prywes R. Expression profiling of serum inducible genes identifies a subset of SRF target genes that are MKL dependent. BMC Mol Biol 2004;5:13.
45. Farshid G, Pradhan M, Goldblum J, Weiss SW. Leiomyosarcoma of somatic soft tissues: a tumor of vascular origin with multivariate analysis of outcome in 42 cases. Am J Surg Pathol 2002;26:14–24.

Cancer Research
The Journal of Cancer Research (1916–1930) | The American Journal of Cancer (1931–1940)

AACR American Association for Cancer Research

Strong Smooth Muscle Differentiation Is Dependent on Myocardin Gene Amplification in Most Human Retroperitoneal Leiomyosarcomas

Gaëlle Pérot, Josette Derré, Jean-Michel Coindre, et al.

Cancer Res 2009;69:2269-2278. Published OnlineFirst March 10, 2009.